ON FATIGUE BEHAVIOR OF SMALL CRACKS INDUCED BY FOREIGN-OBJECT DAMAGE IN TI-6AL-4V

MIRCO D. CHAPETTI
INTEMA – Institute for Materials Science and Technology,
Mar del Plata University. J.B. Justo 4302, (B7608FDQ) Mar del Plata, Argentina

ABSTRACT

A threshold curve method previously developed was applied to analyze the high-cycle fatigue threshold of small cracks induced by foreign-object damage (FOD) in Ti-6Al-4V alloy for which experimental results can be obtained from recent publications. Experimental results found in the literature showed that the small cracks induced by FOD in Ti-6Al-4V alloys could propagate at ΔK as small as 1 MPa $m^{1/2}$, i.e., well below the "worst-case" ΔK_{thR} threshold of 1.9 MPa $m^{1/2}$ for long cracks in this alloy (load ratio R=0.95). According to the results obtained in the present work the threshold for propagation of small cracks (≥20μm) can be as small as 0.8 MPa $m^{1/2}$ considering a stress ratio R = 0.8, for which the threshold for long cracks is about 2.3 MPa $m^{1/2}$. Further, the minimum stress ratio R at which the analyzed cracks can propagate seems to be about 0.6, for which the threshold for large cracks is about 2.7 MPa $m^{1/2}$. It is also shown that for microstructurally small cracks the absence of crack closure effect is not the only reason for the observed faster propagation rates and lower propagation thresholds when compared with long cracks.

1 INTRODUCTION

Foreign object damage (FOD) in gas turbine engines is caused by the ingestion of foreign particles such as sand or runaway debris and the subsequent impact against components, and is one of the major causes of their fatigue failure. FOD will generally cause a crater or tear in the impacted component and reduce the fatigue capacity of the material at the location of the impact.

This work attempts to provide a mechanistic basis for evaluating the detrimental effect of foreign object damage in Ti-6Al-4V by applying a threshold curve method recently developed [1], which takes into account the small crack behavior. Previous works [2-5] have emphasized explanation of fatigue performance of small cracks emanating from FOD by using the "worst-case" ΔK_{thR} threshold for long cracks (determined under R -> 1 condition that minimize crack closure), and the El Haddad model [6] for fatigue propagation threshold of small cracks. In this work a different approach is used.

1.1 fatigue growth threshold of small-cracks

It is well known that small cracks will grow up to the first grain boundary, and it is their arrest which defines the fatigue limit. This is a material-based limit (depending on the microstructural characteristic dimension, *d*) as Miller has pointed out [7]. The approach proposed in reference [1] is based in the above concept and estimates the fatigue crack propagation rate as a function of the difference between the applied driving force and the material threshold for crack propagation. The material threshold for crack propagation as a function of the crack length was defined from a depth given by the position *d* of the strongest microstructural barrier (given by the average microstructural dimension), which defines the smooth fatigue limit, as follows [1]:

$$\Delta K_{th} = \Delta K_{dR} + \left(\Delta K_{thR} - \Delta K_{dR}\right)\left[1 - e^{-k(a-d)}\right] \qquad a \geq d \tag{1}$$

For a crack length $a = d$, $\Delta K_{th} = \Delta K_{dR}$, and ΔK_{th} tend to ΔK_{thR} for long cracks. In terms of the threshold stress, we get:

$$\Delta\sigma_{th} = \frac{\Delta K_{dR} + (\Delta K_{thR} - \Delta K_{dR})[1 - e^{-k(a-d)}]}{Y\sqrt{\pi\, a}} \qquad a \geq d \tag{2}$$

Where ΔK_{thR} and $\Delta\sigma_{eR}$ (and so ΔK_{dR}), are all function of the stress ratio R. The microstructural threshold for crack propagation, ΔK_{dR}, is defined by the smooth fatigue limit $\Delta\sigma_{eR}$ and the position d of the strongest microstructural barrier, as follows:

$$\Delta K_{dR} = Y\, \Delta\sigma_{eR}\, \sqrt{\pi\, d} \tag{3}$$

where Y is the geometrical correction factor. In most cases the initiated microstructurally-small cracks can be considered semicircular [7-9], and the value of Y could then be 0.65. Further, a total extrinsic threshold for crack propagation, ΔK_{CR}, is defined by the difference between the crack propagation threshold for long cracks, ΔK_{thR}, and the microstructural threshold, ΔK_{dR}, function of the crack length. The parameter k can be estimated as a function of the same microstructural and mechanical parameter used to define the material threshold to crack propagation ($\Delta\sigma_{eR}$, d and ΔK_{thR}), as follows

$$k = \frac{1}{4d}\frac{\Delta K_{dR}}{(\Delta K_{thR} - \Delta K_{dR})} = \frac{1}{4d}\frac{\Delta K_{dR}}{\Delta K_{CR}} \tag{4}$$

1.2 application to high-cycle fatigue of foreign object damage

The threshold curve defined by expression (1) or (2) was applied to analyze results of recent studies [2-5] on high-cycle fatigue properties of an α+β processed Ti-6Al-4V blade alloy, where Foreign Object Damage (FOD) was simulated using high-velocity impacts of steel shot on a flat surface. In those studies FOD was simulated by firing 3.2 mm Cr hardened steel spheres normally on to a flat specimen surface of uniaxial fatigue specimen, using a compressed-gas gun facility [3,4]. Figure 1 shows schematically illustration of the cross section of simulated FOD crater after impact [2-5]. A pronounced pile-up of material at the crater rim resulted in multiple microcracking. The mechanistic effect of FOD was considered in terms of [2-5]: (1) the possibility of microcrack formation in the damage zone, (2) the stress concentration associated with the shape of the impact crater, (3) microstructural damage from FOD-induced plastic deformation, and (4) the presence of localized tensile residual hoop stresses in the vicinity of the impact site. Although all of these factors play an important role under certain conditions, in the case of high impact velocities (300 m/s) the formation of damage-induced microcracks, which are formed in the pile-up of materials around the rim, can act as preferred sites for propagating fatigue cracks. When applied stresses are large compared to the impact-induced tensile residual stresses, and in the presence of relatively large (~10-25 μm) impact-induced microcracks, high-cycle fatigue failures (within 10^5-10^6 cycles) initiate directly at the impact site and lead to short fatigue lives. In contrast, at low-applied stresses relative to the residual stresses, high-cycle fatigue failures (after 10^7-10^8 cycles) initiate in locations away from the impact site at regions of peak tensile residual stress, and the necessity for crack nucleation leads to longer fatigue lives.

It has been found that FOD-initiated microcracks, together with the stress concentration of the indent, were the prime reasons that the HCF failures initiated at the FOD sites [2-5]. The microcracks (some as small as 1 μm) grew at applied stress intensities as low as $\Delta K = 1$ MPa $m^{1/2}$, which is well below the "worst-case" ΔK_{thR} threshold in this materials [2] of 1.9 MPa $m^{1/2}$ based on the propagation of large cracks (macroscopic "homogeneous continuum-sized" cracks which are considerably larger than the

scale of the microstructure and for which the threshold for crack propagation is independent of crack length). This worst-case threshold had previously been defined at elevated mean loads (or load ratios, i.e. the ratio of minimum to maximum loads, of about R = 0.95) in an attempt to eliminate effects of closure and to provide a lower-bound threshold for propagation [2]. However, it is clear that this threshold is only relevant to cracks larger than 10-20 times the scale of the microstructure *d* [1], i.e., about 200-400 μm length in the current microstructure (*d* = 20 mm, see Table 1). Since the microcracks associated with impact damage are more than an order-of-magnitude smaller than this, an alternative approach was then proposed to describe the threshold HCF conditions in the presence of FOD [4]. This approach was based on a Kitagawa-Takahashi diagram where the limiting conditions for failure in this case were defined in terms of the smooth fatigue limit (at microstructurally small crack sizes) and the "worst-case" threshold for long cracks.

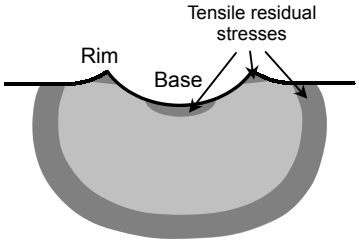

Figure 1. Schematic illustration of the cross section of simulated FOD crater after impact [4].

Finally, in a recent publication [5] the same authors provide a methodology to describe the limiting threshold conditions for failures at both low- and high-applied cyclic stresses. To achieve that, the magnitudes of the residual stresses in the vicinity of various damage sites were computed numerically [10] and measured experimentally using spatially resolved synchrotron X-ray diffraction [11]. Results have shown that prior to fatigue cycling peak tensile values of these residual stresses are on the order of 300 MPa and are located in the interior adjacent to the highly deformed region beneath the indentations (see schema in Figure 1). It was found that for the group of failures observed at 10^7-10^8 cycles and initiated at locations remote from impact damage in regions of high tensile residual stresses, simple superposition of the initial tensile residual stresses onto the applied stresses provided a significant contribution to the reduction in fatigue strength by affecting the local mean stress and load ratio. Accordingly, the modified Kitagawa-Takahashi approach proposed for HCF failures under high-applied stresses must be additionally corrected for the presence of tensile residual stresses to account for failures under low-applied stresses.

In the present work the Chapetti's threshold curve method [1] is applied to analyze the high-cycle fatigue behavior and threshold conditions of the above mentioned FOD-induced microcracks.

2 DATA AND PROCEDURE

1.1. Applied driving force

In the case of small cracks at the indentation rim, an expression for the stress concentration as a function of crack length is needed, that is to say, the normalized applied stress distribution defined by the notch has to be known. Total applied driving force for those small cracks were estimated [2-5] using the expression obtained by Lukas *et al* [12]. For a bimodal Ti-6Al-4V alloy, growing fatigue cracks had an approximate semi-elliptical shape (a ≈ 0.45 c) [3], so that the parameter *Y*, that accounts for the stress-intensity boundary and crack shape corrections, results to be 0.7 [13]. For those cracks growing from smooth surface at locations remote from impact damage in regions of high tensile residual stresses,

expression (7) with $\rho = \infty$ and $k_t = 1$ can be used.

1.2. Data

Results for smooth fatigue limits ($\Delta\sigma_{eR}$) over a range of load ratios from R = 0.1 to 0.8 were obtained from reference [4,14,15]. All data correspond to Ti-6Al-4V with the following chemical composition (%): 6.3Al, 4.19V, 0.19Fe, 0.19O. Mechanical properties: E=110GPa, $\sigma_{0.2}$=915Mpa, σ_{UTS}=965MPa, Elongation:19%, and RA:45%. ΔK_{thR} values were obtained from references [2] and [4]. Microstructural dimension *d* of the material was considered to be equal to the primary α phase size, which has an average diameter of 20 μm [3]. Position and length of initial cracks due to FOD were obtained from references [3], [4] and [5]. Surface length 2c were considered to have an aspect ratio a/c = 0.45.

1.3. Residual stresses

Although the FOD-induced residual stresses do not change ΔK, they do affect the mean stress and hence, alter the effective stress ratio. Thus, the residual stresses should be quantified in order to estimate the effective stress ratio. It was previously shown that the initial residual stress state is reduced by relaxation or redistribution during subsequent fatigue cycling [11]. If the redistribution or first cycle relaxation of the residual stresses are considered, the maximum residual stresses at the time of crack propagation is about 260 MPa. By superimposing a tensile residual stress to the applied stress near fatigue limit the R-ratio increases from 0.1 to ~0.5 and from 0.5 to ~0.7 assuming no relaxation, and from 0.1 to ~0.4 and from 0.5 to ~0.65 assuming relaxation. There are conditions, however, where relaxation does not occur or substantial residual stresses are stable during cycling. Most specifically, the rate and extent or relaxation is a function of the applied stresses.

3 RESULTS AND DISCUSSIONS

Figure 2 shows the near-threshold fatigue growth rates (dashed lines) estimated for small cracks initiated in notched material ($k_t = 1.25$, $\rho = 1.6$ mm) for three different R ratio (0.1, 0.5 and 0.8), as a function of ΔK. The dotted lines show the microstructural thresholds, ΔK_{dR}, which represents the minimum ΔK for crack propagation for a ≥ d at a given R value. FOD-initiated small-crack growth rates are aligned approximately between the large-crack data (lower bound) and naturally-initiated crack data (upper bound). The large-crack threshold of ~1.9 MPa m1/2 at R = 0.95 (where the effect of crack closure is eliminated) has been considered to be a lower bound "worst-case" threshold for cracks of dimensions large compared with the scale of the microstructure [2]. However, smaller FOD-initiated cracks (a ≈ 2-25 μm), comparable with microstructural size-scale, could propagate at stress intensities well below this "worst-case" threshold for long cracks.

Figure 3 shows the influence of crack size on fatigue thresholds in the form of a Kitagawa-Takahashi diagram. It shows the threshold (upper dashed line) defined by the El Haddad threshold stress range as a function a crack length, as proposed in reference [4] for cracks propagating from indent rim at applied R = 0.1. Square symbols correspond to cracks initiated also from the indentation rim but at an applied stress ratio R = 0.5. Triangles symbols correspond to cracks initiated far from the indent, at places with high residual stresses and applied R = 0.1. For these two cases an alternative approach was then proposed [5] using El Haddad model and the smooth fatigue limit as a function of the stress ratio (lower dashed lines). However, the threshold for long crack was considered to be equal to 1.9 MPa $m^{1/2}$ ("worst case", R = 0.95,) for all curves, that is to say, for all stress ratio. Unless a gradient in residual stress is considered, the smooth fatigue limit and the threshold for long cracks should correspond to the same R-ratio. The threshold curve defined by using the El Haddad model, with the smooth fatigue limit for R=0.1 and the "worst-case" threshold for long cracks, gives a threshold stress of about 330 MPa for a crack length $a = d$, that is to say, a difference of about 120 MPa can be observed (about 30%).

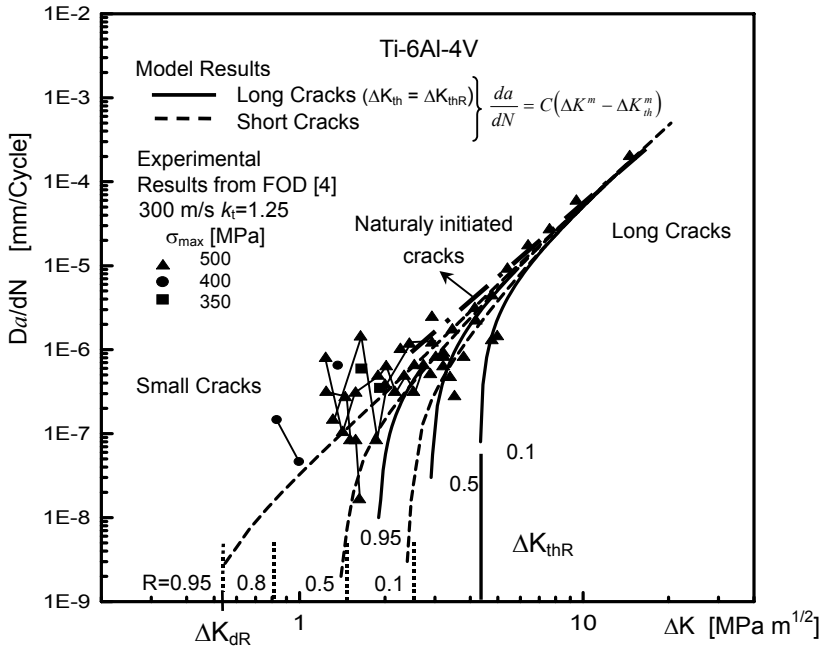

Figure 2. Fatigue crack propagation rates

Figure 3 also shows the estimated threshold stress curves. In the case of cracks initiated far from the rim at applied R = 0.1, the effective R-ratio is about 0.5 due to the residual stresses. The estimated threshold stress curve for R=0.6 could explain all failures for this case, but the fatigue limit for R=0.5 (300 MPa) could also be a good estimation of the average result. For failures due to cracks initiated from the indentation rim for R = 0.5, the effective R-ratio is about 0.65 due to residual stresses, and the estimated threshold curve for R=0.6 can explain failure for these cases. For failure due to crack initiated from the indentation rim but for R = 0.1, and considering that the residual stresses are partially relaxed, the effective applied R-ratio is about 0.4.

5 CONCLUDING REMARKS

The threshold curve defined by using the El Haddad model, the smooth fatigue limit for R=0.1 and the "worst-case" threshold for long cracks, gives a threshold stress of about 30% smaller than the smooth fatigue limit for a crack length $a = d$. This is in contradiction with the experimental evidence that smooth fatigue limit is usually given by the resistance of the stronguest microstructural barrier, placed at $a = d$. To clarify this uncertainty the threshold stress for microstructurally-small cracks of about 20 μm in undamaged and smooth material should be analyzed experimentally. For reliable threshold estimations the deterioration of the smooth fatigue limit due to the microstructural damage should be study and quantified.

The threshold for small crack propagation could be as small as 0.8 MPa $m^{1/2}$ considering a stress ratio R = 0.8, for which the threshold for large cracks is about 2.3 MPa $m^{1/2}$. The minimum stress ratio R at which the analyzed cracks could propagate is about 0.6, for which the threshold for large cracks is about 2.7 MPa $m^{1/2}$. These results show that for microstructurally small cracks the absence of crack closure

effect is not the only reason for the observed faster propagation rates and lower propagation thresholds when compared with long cracks.

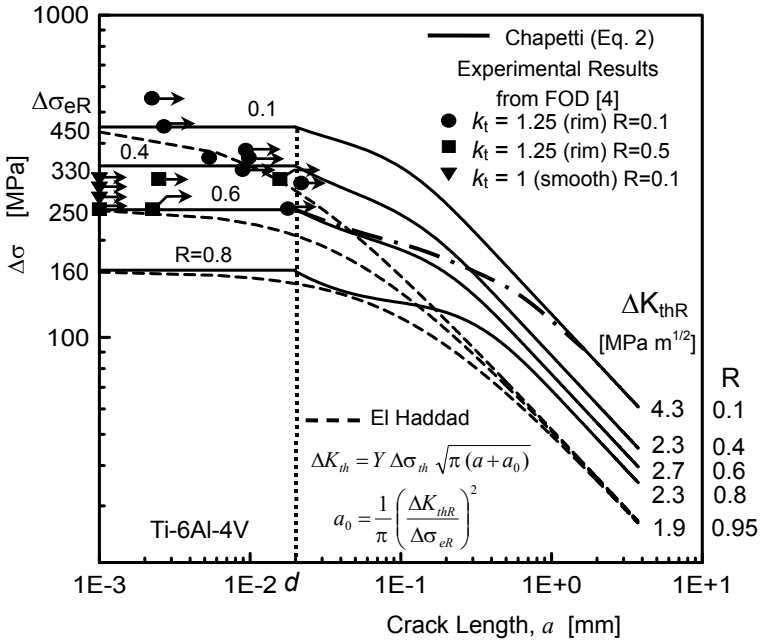

Figure 3. Kitagawa-Takahashi diagram

References

[1] Chapetti M.D. International J. of Fatigue Vol.25, No12, pp.1319-1326, 2003.

[2] Ritchie RO, Davison DL, Boyce BL, Campbell JP and Roder O. Fat Fract Engng Mat Struct Vol.22, pp.621-631, 1999.

[3] Peters JO, Roder O, Boyce BL, Thompson AW and Ritchie RO. Metallurgical and Materials Transactions A Vol.31, pp.1571-1583, 2000.

[4] Peters JO, Ritchie RO. Materials Science and Engineering A Vol.319-321, pp.597-601, 2001.

[5] Peters JO, Boyce BL, Chen X, McNaney JM, Hutchinson JW and Ritchie RO. Engng Fract Mech Vol.69, pp.1425-1446, 2002.

[6] El Haddad MH, Topper TH and Smith KN. Engng. Fract. Mech. Vol.11, pp.573-584, 1979.

[7] Miller KJ. Fat Fract Engng Mater Struct 16(9), 931-939, 1993.

[8] Taylor D and Knott JK. Fat. Engng. Mater. Struct Vol.4, No.2, pp.147-155, 1981.

[9] Lankford J. Fat. Engng. Mater. Struct., Vol.8, No.2, pp.161-175, 1985.

[10] Chen X and Hutchinson JW. Int. J. Fracture Vol.107, pp.31-51, 2001.

[11] Boice BL, Chen X, Hutchinson JW and Ritchie RO. Mech. of Mater Vol.33, pp.441-454, 2001.

[12] Lukás P, Kunz L, Weiss B and Stickler R (1989) *Fat Fract Engng Mater Struct* Vol.12 No3, pp.175, 1989.

[13] Newman Jr JC. and Raju IS. Engng. Fract. Mech. Vol.15 (1981), pp.185-92.

[14] Hines JA, Peters JO and Lütjering G. In: Boyer, Eylon and Lütjering, editors. Fatigue behaviour of titanium alloys, Warrendale, PA: TMS; 1999, pp.15-22.

[15] Bellow RS, Muju S and Nicholas T. Int. J. Fatigue Vol.21 (1999), pp.687-97.